NPHS2, encoding the glomerular protein podocin, is mutated in autosomal recessive steroid-resistant nephrotic syndrome

Nicolas Boute[1], Olivier Gribouval[1], Séverine Roselli[1], France Benessy[1], Hyunjoo Lee[1], Arno Fuchshuber[1], Karin Dahan[3], Marie-Claire Gubler[1], Patrick Niaudet[2] & Corinne Antignac[1]

Familial idiopathic nephrotic syndromes represent a heterogeneous group of kidney disorders, and include autosomal recessive steroid-resistant nephrotic syndrome, which is characterized by early childhood onset of proteinuria, rapid progression to end-stage renal disease and focal segmental glomerulosclerosis. A causative gene for this disease, *NPHS2*, was mapped to 1q25–31 and we report here its identification by positional cloning. *NPHS2* is almost exclusively expressed in the podocytes of fetal and mature kidney glomeruli, and encodes a new integral membrane protein, podocin, belonging to the stomatin protein family. We found ten different *NPHS2* mutations, comprising nonsense, frameshift and missense mutations, to segregate with the disease, demonstrating a crucial role for podocin in the function of the glomerular filtration barrier.

Introduction

Plasma ultrafiltration during primary urine formation in the glomerulus is a central function of the kidney. The structurally complex glomerular capillary wall is responsible for this function and is composed of a basement membrane covered by fenestrated endothelium on the inner surface and highly specialized epithelial cells called podocytes (due to their characteristic interdigitated foot processes, on the outer surface). Dysfunction of the glomerular filter, resulting in extensive leakage of plasma proteins and diffuse effacement of podocyte foot processes detected by electron microscopy, is observed in many acquired and inherited nephropathies. The clinical hallmark is nephrotic syndrome characterized by heavy proteinuria, edemas, hypoalbuminaemia and hyperlipidaemia. Progression to end-stage renal disease (ESRD) is associated with the development of focal segmental glomerulosclerosis[2] (FSGS).

The study of genetic diseases with filtration barrier defects provides useful models for deciphering the physiopathology of the glomerular filtration process. The most severe such disorder is congenital nephrotic syndrome of the Finnish type (CNF), caused by mutations in the recently identified gene *NPHS1* (ref. 3). *NPHS1* encodes a transmembrane protein of the Ig superfamily called nephrin[3], which is exclusively localized at the slit diaphragm joining the interdigitated podocyte foot processes[4–6]. Less severe cases of familial proteinuria or nephrotic syndrome with FSGS have also been described. These forms have an adult onset and a slow progression towards renal failure. Two loci for autosomal dominant forms of these 'familial' FSGS have been mapped to 19q13 (ref. 7) and 11q21–q22 (ref. 8), respectively, but the underlying genes have not yet been identified.

Previously, we delineated a new type of familial steroid-resistant idiopathic nephrotic syndrome (SRN; MIM 600995) characterized by an autosomal recessive mode of inheritance, onset between three months and five years, resistance to steroid therapy, rapid progression to ESRD, absence of recurrence after renal transplantation and absence of extra-renal disorders. Histologically, minimal glomerular changes are observed on early biopsy samples and FSGS is present at later stages. Although we demonstrated genetic heterogeneity in this subset of patients, we mapped a gene for SRN, *NPHS2* (formerly *SRN1*), to 1q25–q31 between the markers *D1S452* and *D1S466*, a region spanning approximately 12 cM (ref. 9).

Here we use positional cloning to identify the causative gene. We found that *NPHS2* is exclusively expressed in the podocytes and encodes an integral membrane protein, which we named podocin.

Results

Physical mapping of the candidate region and refinement of the *NPHS2* interval

By linkage analysis of our previously reported families using new microsatellite markers[10] as well as analysis of novel families, we refined the *NPHS2* locus between the markers *D1S480* and *D1S2883*, a region of 2.7 cM. A YAC contig (20 clones) spanning this region was retrieved from the Whitehead Institute server. Using the sequence-tagged site (STS) content provided by various databases and YAC-end sequences as new STSs, we constructed a PAC contig spanning the *NPHS2* interval, with five gaps partially bridged by cosmid clones. A renewed linkage analysis of two consanguineous families (8 and 10) using new microsatellite markers (*D1S1640*, *D1S3758*, *D1S3760*, *D1S215* and *D1S3759*) assigned to the contig (Fig. 1) localized the SRN locus between the markers *D1S1640* and *D1S3759*, an interval estimated at 2.5 Mb.

We assigned ESTs belonging to 14 UniGene clusters, 5 independent ESTs, 4 known genes (*NGAP*, *SOAT1*, *ABL2* and *KIAA0475*) and 1 pseudogene (*RPS14P1*) to the contig (Fig. 1). The four genes encode a Ras GTPase activating protein; an acyl-CoA:cholesterol acyltransferase; a tyrosine-protein kinase; and an unknown protein, KIAA0475, respectively. As we found *NGAP*

[1]*Inserm U423, Tour Lavoisier and* [2]*Service de Néphrologie Pédiatrique, Hôpital Necker-Enfants Malades, Université René Descartes, Paris, France.* [3]*Center for Human Genetics, University of Louvain Medical School, Bruxelles, Belgium. Correspondence should be sent to C.A. (e-mail: antignac@necker.fr).*

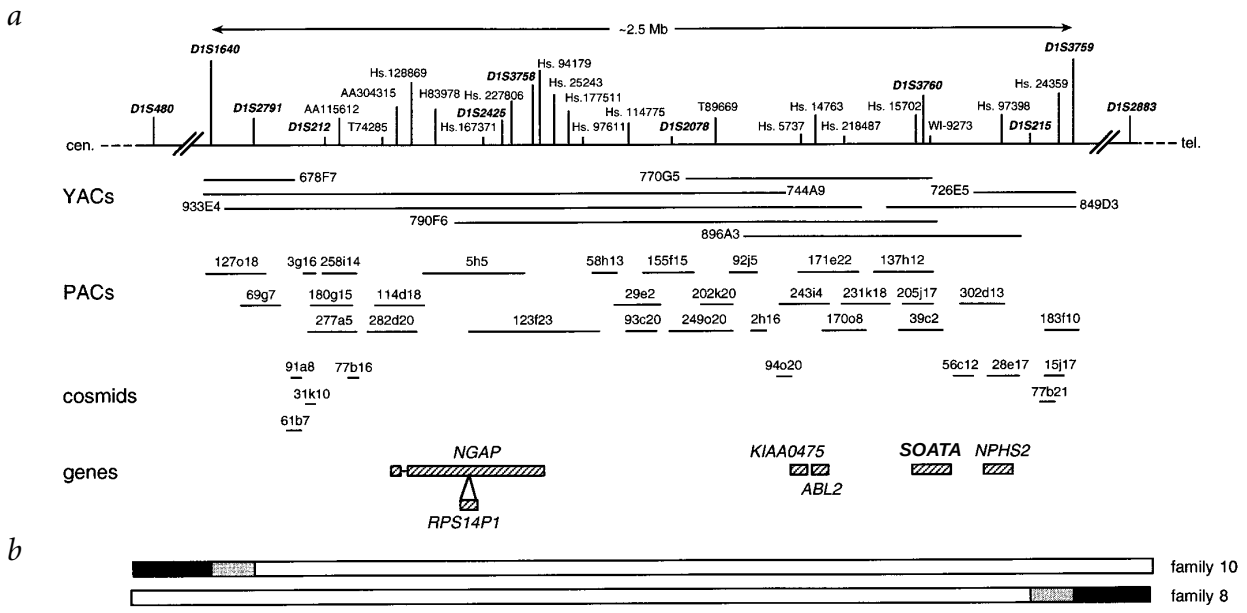

Fig. 1 Map of the *NPHS2* region. ***a***, Physical map of the *NPHS2* interval. The 2.5-Mb candidate region is delineated by the markers *D1S1640* and *D1S3759*. The map position of polymorphic markers and STSs (in bold and italics) and single ESTs and UniGene clusters of ESTs is indicated. YACs, PACs and cosmids are represented by lines. Genes are indicated by hatched boxes. *NGAP* is represented by two boxes separated by a horizontal line, which symbolizes the presence of 5′ alternatively spliced exons, probably due to an alternative promoter. *RPS14P1*, a pseudogene of the ribosomal protein S14, is located inside a *NGAP* intron. The UniGene clusters Hs. 14763 and Hs. 15702 were assigned to the 3′ UTR of the genes *ABL2* and *SOAT1*, respectively, by RACE–PCR and screening of kidney cDNA libraries. ***b***, Schematic representation of crucial recombination events in families 8 and 10. The recombinant haplotypes are symbolized by filled boxes, and regions of homozygosity and crossing-over events by open and grey boxes, respectively.

and *KIAA0475* to be expressed in kidney as well as other tissues by northern-blot analysis (data not shown), we undertook mutation screening in nine affected individuals. We detected no pathogenic mutations in the regions tested. *SOAT1* and *ABL2*, as well as three ESTs and four UniGene clusters that were not expressed in kidney, were not further analysed. The remaining UniGene clusters and EST were considered for further analysis.

Identification of *NPHS2*

We localized the EST AA398634, belonging to one of these UniGene clusters (Hs. 97398) and mapping to the BAC clone 545A16 (The Sanger Centre, United Kingdom), to the cosmid 28e17 and PAC 302d13 clones of the contig (Fig. 1). Using RT–PCR we found that this EST, originating from an adult testis library, was also expressed in kidney. By 5′-and 3′-RACE–PCR of a human fetal kidney adaptator-ligated cDNA library, a transcript with a putative ORF and homology with six known ESTs (UniGene cluster Hs. 192657), all from a kidney cDNA library, was amplified. Subsequent screening of a human fetal kidney cDNA library allowed the reconstitution of a 1,853-bp transcript. The five isolated cDNA clones start between positions 1 and 5 of the reconstituted cDNA sequence and contain a methionine codon located 70 nt downstream from the first nucleotide. This ATG codon lies within a Kozak translation initiation consensus sequence[11]. Sequence analysis of 710 bp of genomic sequence upstream of the ATG codon, using the programs TSSG and TSSW (ref. 12), predicted the presence of a transcription start site located 83 bp upstream of the ATG codon (TSSG and TSSW scores of 21.97 and 13.08, respectively). These features suggested that this ATG is the translation initiation codon. The complete *NPHS2* ORF is 1,149 bp and is followed by a 635-bp 3′ UTR containing an atypical polyadenylation signal (AATTAAA) situated 13 nt upstream of the poly(A) tail. The sequence of the EST AI672038 (belonging to the UniGene cluster Hs.192657), however, shows that one of two overlapping consensus polyadenylation signals (AATAAA) located 44 bp downstream of the aforementioned signal can also be used.

The length of the isolated cDNA sequence is in agreement with the size of the transcript (~2 kb) detected by northern-blot analysis. The transcript was strongly expressed in human fetal and adult kidney with no signal being observed in other tissues (Fig. 2*a*,*b*). This was further confirmed by hybridization of a normalized human poly(A)$^+$ RNA dot blot containing RNA from 50 different human tissues. We observed a strong hybridization signal in mature and fetal kidney, whereas a weak signal in the adult testis, fetal heart and fetal liver was seen only after a 24-hour exposure (Fig. 2*c*). The expression pattern suggested that this gene was likely to be *NPHS2*.

Screening for mutations

We next amplified total RNA from an end-stage kidney of an affected member of family 8 using RT–PCR with cDNA-specific primers. We observed a barely detectable amplification product (Fig. 3*a*), suggesting that the transcript of interest was expressed at a very low level due to a mutation in the corresponding gene. We determined the gene structure by sequencing DNA from the cosmid 28e17 and PAC 302d13 clones using cDNA-specific primers (see Table 1, http://genetics.nature.com/supplemetary_info/), screened the 8 coding exons and intron-exon junctions of 16 unrelated affected individuals for mutations by SSCP, and detected 10 different mutations in 14 families (Table 2). All mutations co-segregated with the disease, and none were identified in 80 control chromosomes. Three mutations resulted in a frameshift or a premature stop codon (Fig. 3*b*,*c*), potentially null mutations. Six were missense mutations. Of these, two (R138Q and V180M), which occur in a CpG pair, were detected in unrelated families. We found R138Q in the heterozygous state in two families (4 and 12) and in the homozygous state in four families with no known consanguinity (families 6, 7, 11 and 13). Five of

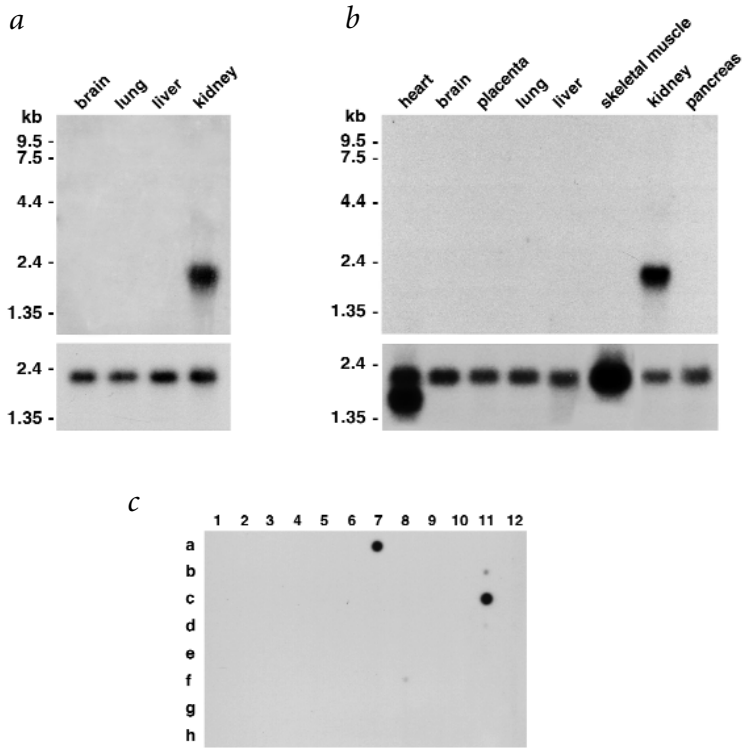

Fig. 2 Tissue distribution and relative expression of *NPHS2* in human tissues. Northern-blot analysis is shown of human fetal poly(A)+ RNA (***a***) and human adult poly(A)+ RNA (***b***) by hybridization of a 1,065-bp *NPHS2* probe spanning exons 5–8 (top) and a β-actin specific probe as a loading control (bottom). ***c***, Northern dot-blot analysis of human fetal and adult poly(A)+ RNA of 50 different tissues by hybridization of the same *NPHS2* probe. A signal can be seen at positions a7, f8, b11, c11 and d11 corresponding to poly(A)+ RNA from adult kidney and testis, and fetal heart, kidney and liver, respectively. Rehybridization of the dot blot with the ubiquitin probe confirmed the normalized loading of RNA samples (data not shown).

these patients originated from Germany or The Netherlands. The mutation was not found in 28 additional control DNA samples from unrelated individuals from these countries. These data indicated that this gene was indeed *NPHS2*.

Characterization of the protein product of *NPHS2*

The full-length *NPHS2* cDNA encodes a putative 383–amino-acid protein of approximately 42 kD, which we named podocin. Database comparisons of this sequence detected a region of extensive similarity between the central region of podocin and proteins of the band-7-stomatin family. The band-7-stomatin protein family signature was found between amino acids 238 and 266 of podocin by comparison with the Prosite database[13]. The strongest homologies were found with human stomatin (47% identity and 67% similarity over 253 aa) and *Caenorhabditis elegans* MEC-2 (44% identity and 65% similarity over 275 aa; Fig. 4). Analysis of the podocin amino-acid sequence using the PSORTII program[14] suggested that *NPHS2* encodes an integral membrane protein with one transmembrane domain (aa 105–121) and a 262–amino-acid carboxy-terminal cytoplasmic tail. The transmembrane domain and most of the cytoplasmic tail are homologous to the corresponding regions of the stomatin family proteins. Furthermore, the cysteine residue located four amino acids upstream of the transmembrane domain, which is conserved among stomatins and MEC-2 and has been shown to be the major palmitoylation site in stomatin[15], was also conserved in podocin. Podocin, however, extends beyond the stomatin-like sequences at both the N and C termini (97 aa and 36 aa, respectively), which show no homology with any known protein sequence.

In situ hybridization

We performed *in situ* hybridization on normal fetal and postnatal kidney samples using digoxigenin- or [^{35}S]-labelled riboprobes (Fig. 5). We observed strong signals exclusively in glomeruli. In the fetuses, no signal was detected in the earlier stages of nephron development, whereas intense signals were seen in the future podocytes of the inferior segment of the S-body, concomitant with vascularization of the inferior cleft (Fig. 5*a*). This expression was maintained at the same level in immature glomeruli and persisted in mature glomeruli of the deep cortex (Fig. 5*c*). All glomeruli were still strongly labelled in post-natal kidneys. Under high magnification, transcript expression was restricted to within the podocytes, at the periphery of the glomerular tuft (Fig. 5*b*,*d*). No specific signals were obtained with the sense probes (Fig. 5*e*).

Discussion

Here we identified by positional cloning a new gene, *NPHS2*, which is mutated in a subset of childhood steroid-resistant nephrotic syndrome with FSGS. This gene was identified by characterization of ESTs in the critical interval at 1q25–q31 and considered to be a candidate gene due to its almost exclusive expression in fetal and mature kidney. The detection of mutations leading to premature termination of the protein in affected individuals confirmed it as the causative gene.

NPHS2 encodes a new member of the stomatin protein family, which we named podocin due to the specific expression of *NPHS2* in podocytes. Stomatin, also known as band-7 protein, is an integral membrane phosphoprotein initially isolated from erythrocyte plasma membranes and subsequently found to have a more widespread expression[16]. Its function has not yet been determined. Like MEC-2, another member of this family which is required for the function of touch-receptor neurons in *C. elegans*[17], it has been suggested to have a role in primary sensory neurons by linking ion channels to the cytoskeleton[17,18].

Podocin has a structure similar to that of all stomatin-like proteins, which consists of an N-terminal domain, a short transmembrane domain and a cytosolic C-terminal domain. Both the N- and C-terminal domains of stomatin and MEC-2 are cytosolic[17,19], suggesting that their transmembrane domains form a hairpin-like structure. Stomatin forms homo-oligomeric complexes via its C terminus[20]. This oligomerization, coupled with the presence of palmitoylated cysteine residues, is thought to greatly increase the affinity between stomatin and the plasma membrane[15]. Given the sequence homology between stomatin and podocin, a similar monotopic conformation might be predicted for podocin. Other integral membrane proteins, such as caveolins, possess a hairpin-like membrane domain and form homo-oligomers[21]. Due to the side-by-side interactions of these oligomers, resulting in the formation of complex structures, caveolin is thought to act as scaffolding in membrane of caveolae[21]. These elements suggest that podocin may form homo-oligomers resulting in a widespread structure which, in turn, may interact with other podocyte proteins and function as a linker between the plasma membrane and the cytoskeleton.

Although the subcellular localization of podocin is not yet known, it is tempting to speculate that it might interact directly or indirectly with nephrin, which is involved in CNF (ref. 3). It has

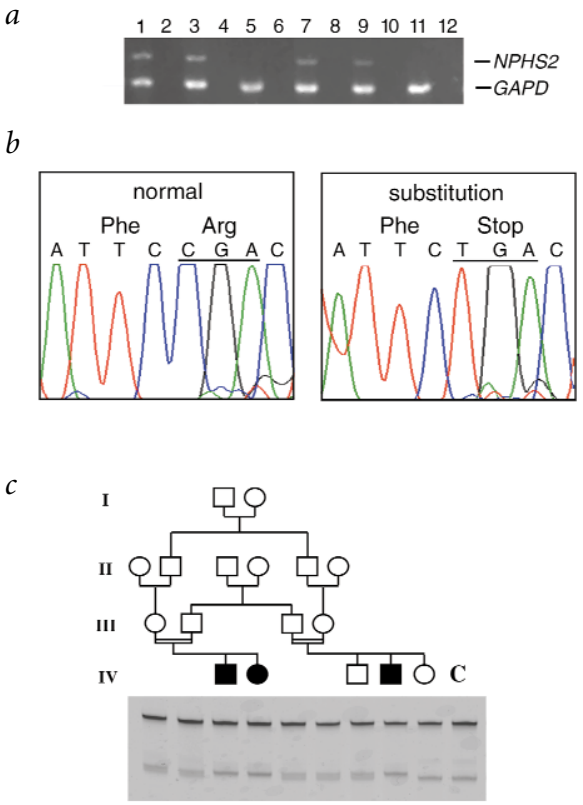

Fig. 3 Detection of *NPHS2* mutations. ***a***, RT–PCR analysis of *NPHS2* expression. A barely detectable product was amplified using the End Stage Renal Disease (ESRD) kidney from an affected member from family 8 (lane 5) and no product was amplified from normal adult liver RNA (lane 11). As positive controls, products of the expected size were amplified using RNA from normal fetal and mature kidneys (lanes 1, 3) as well as from non-SRN end-stage renal kidneys (lanes 7,9). In contrast, there was no significant difference in the intensity of the co-amplified *GAPD* fragments. As a negative control (even-numbered lanes), MMLV reverse-transcriptase was not added to the reverse transcription reaction. ***b***, Detection of mutations by direct sequencing. Detection of homozygous C→T substitution in exon 3 at position 412, resulting in a premature TGA stop codon at aa 138 (R138X) in an affected individual of family 8. ***c***, Segregation of the R138X mutation with the disease phenotype in family 8. By SSCP analysis a homozygous band pattern different from that of the control individual was detected in three affected individuals (IV-1, 2 and 4), whereas the four unaffected parents (III-1, 2, 3 and 4) and the unaffected son (IV-3) display a heterozygous mutation pattern. A SSCP pattern identical to that of the control was generated by tissue from the unaffected daughter (IV-5).

recently been shown that nephrin can associate with CMS (known as Cd2ap in mice) at the slit diaphragm of podocyte foot processes[22,23]. CMS is an adapter molecule involved in cytoskeletal rearrangement and, when inactivated, results in a congenital nephrotic syndrome in the mouse[22]. In contrast, no direct interactions were found between nephrin and ZO-1 despite the fact that they are both localized at the slit diaphragm[5]. Thus, podocin may have a role in stabilizing interactions between these proteins and anchoring them to the cytoskeleton. Along this line, the podocin C terminus contains six proline residues that may be SH3-binding sites and may therefore interact with one SH3 domain of CMS. Another possibility is that podocin interacts with the focal adhesion proteins involved in cell-matrix interactions at the basolateral membrane of the podocyte. Of note, mice lacking laminin β2 display a nephrotic syndrome (ref. 24).

Regardless of how podocin functions, it has a role in regulating glomerular permeability, as determined by patient phenotype. We have shown, however, that *NPHS2* is expressed early during kidney development in the metanephros, and it remains to be determined why inactivation of *NPHS2* does not lead to a congenital nephrotic syndrome as is the case with *NPHS1*.

We detected *NPHS2* mutations in 14 of 16 families with SRN for which haplotype analysis was compatible with linkage to the *NPHS2* locus. Mutations include premature protein termination as well as missense mutations. The latter are predicted to cause either non-conservative substitutions (P20L, G92C, R291W) or replacement of residues that are highly conserved among the stomatin-like protein family members (R138Q and D160G) and are probably crucial for podocin function. One mutation, G92C, also involves the last nucleotide of exon 1 and probably affects the splicing process. These mutations are therefore expected to be pathogenic. The V180M variant, detected in three affected individuals of different geographic origins involves two non-polar amino acids in a non-conserved amino acid. Its absence from 40 control individual suggests that it is pathogenic.

The R138Q mutation was found in approximately one-third of the patients and, if this prevalence is confirmed using a larger affected population, may be useful in mutation screening. Additional cases need to be tested to clarify whether this mutation is due to a founder effect or recurrent mutation; its occurrence in six families from the same part of Europe favours the former scenario.

Although other loci have been mapped for autosomal dominant FSGS (refs 7,8), *NPHS2* is the first gene involved in familial

Table 2 • Mutations detected in *NPHS2*

Type of mutation	Nucleotide change[a]	Effect on coding sequence	Exon	Family	Mutation status[b]
nonsense	412C→T	R138X	3	8[c]	hom.
frameshift	104/5insG	frameshift	1	14	het.
	419delG	frameshift	3	14	het.
	855/6delAA	frameshift	7	9	het.[d]
missense	59C→T	P20L	1	15[c]	hom.
	274G→T	G92C	1	3	het.[de]
	413G→A	R138Q	3	4	het.[d]
				6	hom.
				7	hom.
				11	hom.
				12	het.
				13	hom.
	479A→G	D160G	4	16[c]	hom.
	538G→A	V180M	5	10[c]	hom.
				12	het.
	871C→T	R291W	7	2	het.[d]

[a]The nucleotides are numbered from the A of the ATG initiation codon[39]. [b]hom., homozygous mutation; het., heterozygous mutation. [c]Consanguineous family. [d]Only paternal mutation detected. [e]Involves the last nucleotide of exon 1 and thus probably also alters splicing.

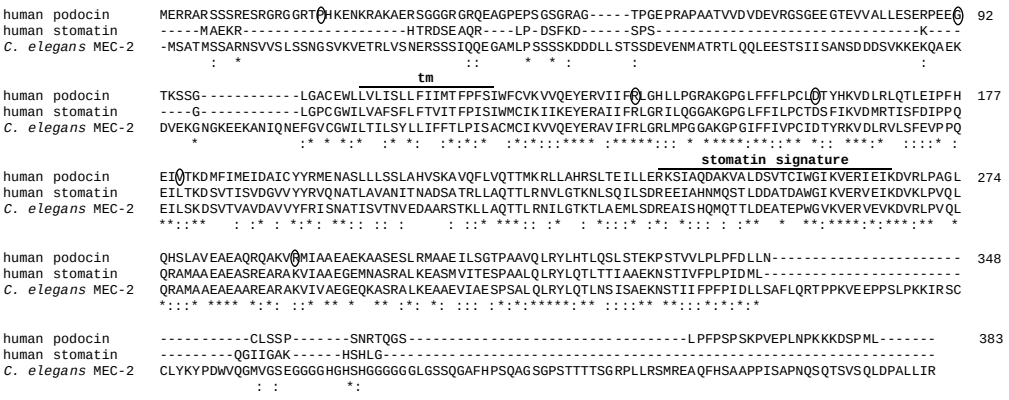

Fig. 4 Amino-acid sequence comparison of human podocin, human stomatin and *C. elegans* MEC-2. Identical residues are indicated by an asterisk *, similar residues, by a colon. The predicted transmembrane (tm) domain and the stomatin signature sequence are overlined. The amino acid residues affected by missense mutations are circled.

FSGS to be identified. It is likely that *NPHS2* mutations will be found in sporadic cases of steroid-resistant idiopathic nephrotic syndrome, which represent an important cause of childhood ESRD. The small number of *NPHS2* exons and the detection of a frequent mutation will allow rapid screening of these individuals for mutation of *NPHS2*. The detection of *NPHS2* mutations is of clinical utility; it would prescribe against unnecessary immunosuppressive therapy and permit the prediction of an absence of disease recurrence after kidney transplantation. Furthermore, it is also possible that *NPHS2* might have a role in the development of secondary FSGS observed in diseases such as diabetic nephropathy[25], HIV nephropathy[26] or morbid obesity[27].

Methods

PAC and cosmid contig construction and isolation of polymorphic markers. A human genomic PAC library (RPCI 1; ref. 28) and a chromosome 1-specific cosmid library (LL01NC01; ref. 29) were provided by the UK HGMP Resource centre. We isolated PAC clones by PCR screening using microsatellite markers, STS and ESTs spanning the chromosomal region between *D1S1640* and *D1S3759*. Cosmid clones were isolated by hybridization of cosmid library filters with probes corresponding to PAC ends. Cosmid and PAC clones were directly sequenced as described[30]. ESTs reported in GeneMap'96 and '98 and those listed in the Sanger Centre database as mapping to the gene interval were assigned to the contig by PCR amplification. *D1S215* and *D1S1640* were retrieved from the Genethon genetic map and the Genome Database, respectively. The *D1S3760* marker is localized within intron 12 of *SOAT1* as described[31]. We identified *D1S3758* and *D1S3759* while sequencing the *NGAP* intron-exon boundaries and *Hin*dIII-*Sac*II subclones of PAC 183f10. PCR amplification of these two markers was carried out using the primers 5′–AACATAAACTCATCCCACC–3′ and 5′–AATAGTAGCTAACT GCCACC–3′ for *D1S3758* and 5′–CTTGTAAAGGCTTAGGAATG–3′ and 5′–AGGCAGTCACAGTAGAGGT–3′ for *D1S3759* at an annealing temperature of 55 °C.

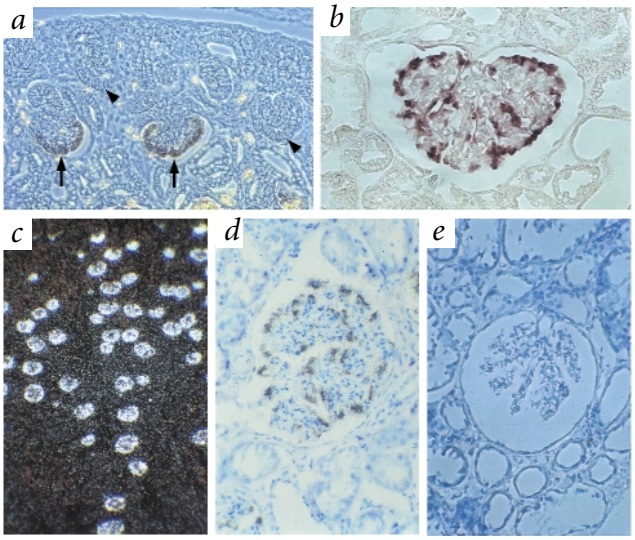

Fig. 5 *In situ* hybridization of antisense (*a*–*d*) and sense (*e*) *NPHS2* riboprobes labelled with digoxigenin (*a*,*b*) or [^{35}S]UTP (*c*–*e*). ***a***, In the superficial cortex of a 12–gestational-week (GW) fetus, strong signals were observed in the developing podocytes of the late S body and the immature glomerulus (arrow), whereas no signal was detected in earlier structures (arrowhead). ***b***, In the mature kidney, the podocytes at the periphery of the glomerular tuft were intensely labelled. ***c***, Dark-field autoradiograph, showing strong signals in all the glomeruli of a 26 GW fetus. ***d***, Bright-field autoradiograph of a mature glomerulus showing the silver grains localized to the podocytes. ***e***, No signal was detected on a bright-field autoradiograph upon hybridization of the sense probe. Magnifications are as follows: *a*, ×150; *b*, ×250; *c*, ×50; *d*,*e*, ×180.

cDNA cloning. We extracted total RNA from human fetal kidney using the RNAeasy Maxi kit (Qiagen) and purified poly(A)$^+$ RNA with the mRNA purification kit (Pharmacia Biotech). We amplified cDNA from human fetal kidney poly(A)$^+$ RNA by several rounds of 5′ and 3′ RACE–PCR using the Marathon cDNA Amplification kit (Clontech) according to the manufacturer's instructions. Primary and nested PCRs were carried out using the adaptor primers (AP1 and AP2) coupled with primers specific to known cDNA sequences. Subsequent rounds of amplification were performed with primers specific to the newly isolated RACE–PCR clones. RACE–PCR amplification products were subcloned using the pGEM-Teasy vector system II (Promega) and the corresponding clones sequenced. To obtain the 5′ region of the *NPHS2* cDNA and to confirm the reconstructed cDNA sequence, we screened a human fetal kidney cDNA library (Clontech) with a 1,065-bp cDNA probe containing the last four exons of *NPHS2* (positions 728 to 1,792).

RT–PCR. We isolated total RNA from human fetal and adult kidney, adult liver and end-stage renal kidneys as described above. After a 30-min incubation with RQ1 DNAse (Boehringer), cDNA synthesis was performed using RNA (5 μg), random primers (600 ng; Promega) and MMLV reverse transcriptase (200 U; Gibco Life Technologies) according to standard procedures. We carried out PCR amplification using *NPHS2* cDNA primers, 5′–AGGTGGTGGCGCTGTTGGAG–3′ and 5′–GAAGCAGATGTCCCA GTCGGAATAT–3′, and *GAPD*-specific primers[32] at an annealing temperature of 58 °C.

Sequence analysis. Nucleotide comparison of the *NPHS2* cDNA sequence and those of known genes and ESTs listed in a non-redundant compilation of the EMBL and GenBank databases were performed using the BLAST program[33]. We carried out amino-acid comparisons with the non-redundant Swiss-Prot database using the BLASTP program. Multiple alignments were performed using CLUSTAL W (ref. 34), protein-domain homologies and motifs predicted using the Prosite database[13], membrane topology using the PSORT program[14] and the PolII promoter sequences using the TSSG and TSSW programs[12].

Genotyping and mutation screening. We obtained blood samples after informed consent from 16 families originating from Europe, North Africa, Egypt, Turkey and Saudi Arabia. Of these families, nine have already been reported, families 2-9 (ref. 9) and family 10 (ref. 35). All patients presented with SRN according to defined criteria[9]. Haplotype analysis was compatible with linkage to the *NPHS2* locus in all families: five were consanguineous and in one additional family (family 13), affected individuals were homozygous for five consecutive markers spanning the *NPHS2* locus. Genotyping of DNA with microsatellite markers was carried out as described[9]. For the SSCP analysis, exons were amplified by PCR using flanking intronic primers. We selected primers and PCR conditions using the Oligo 5.0 program (NBI): exon 1, 5′–GCAGCGACTCCACAGGGACT–3′ and 5′–TCAGTGGGTCTCGTGGGGAT–3′; exon 2, 5′–AGGCAGTGAATACA GTGAAG–3′ and 5′–GGCCTCAGGAAATTACCTA–3′; exon 3, 5′–TTCTG GGAGTGATTTGAAAG–3′ and 5′–TGAAGAAATTGGCAAGTCAG–3′; exon 4, 5′–AAGGTGAAACCCAAACAGC–3′ and 5′–CGGTAGGTAGACCATGGAAA –3′; exon 5, 5′–CATAGGAAAGGAGCCCAAGA–3′ and 5′–TTTCAGCATATTG GCCATTA–3′; exon 6, 5′–CTCCCACTGACATCTGA–3′ and 5′–AATTTAAAAT GAAACCAGAA–3′; exon 7, 5′–CTAAATCATGGCTGCACACC–3′ and 5′–CTT CCTAAAGGGCAGTCTGG–3′; exon 8, 5′–GGTGAAGCCTTCAGGGAATG–3′ and 5′–TTCTATGGCAGGCCCCTTTA–3′; at annealing temperatures of 50 °C (exon 6), 55 °C (exons 2, 3, 4 and 5) and 60 °C (exons 1, 7 and 8). Due to the high GC content of exon 1, we carried out PCR using the Qiagen *Taq* polymerase and Q-Solution according to the manufacturer's instructions. Moreover, due to its size, the PCR product of exon 1 was digested by *Sma*I into two fragments before gel electrophoresis. Electrophoresis was carried out for 2 h at 600 V, 25 mA and 15 W with the Genephor Electrophoresis Unit using the GeneGel Excel 12.5/24 kit (Pharmacia). Staining was performed in a GeneStain Automated Gel Stainer using PlusOne Silver Staining kit (Pharmacia).

***In situ* hybridization.** We paraffin-embedded and sectioned (6 µm) kidneys from three fetuses (12–30 weeks of gestation) and six children or adults (ranging from 1 month to 51 y). After deparaffinization and rehydration, we treated sections by microwave heating in sodium citrate buffer (0.01 M, pH 6) to enhance the hybridization signal. The *NPHS2* riboprobes were synthesized from a 1,065-bp PCR product (spanning bases 728 to 1,792 in the *NPHS2* cDNA) subcloned into the vector PGEM-Teasy (Promega). The antisense probe was synthesized after digestion with *Sal*I using the T7 polymerase and the sense probe after digestion with *Sac*II using the Sp6 polymerase. The riboprobes were labelled with either digoxigenin-11-UTP (Roche) according to the manufacturer's instructions or [^{35}S]UTP as described[36]. *In situ* hybridization was carried out as described for the digoxigenin-11-UTP (ref. 37) and the [^{35}S]UTP-labelled probes (ref. 38).

GenBank accession numbers. *NPHS2* cDNA, AJ279254; exons and flanking intronic regions, AJ279246–AJ279253

Note added in proof: During the publishing process, J. Kaplan *et al.* have shown that mutations in *ACTN4*, mapped to 19q13 and encoding a-actinin-4, an actin-filament cross linking protein, cause autosomal FSGS (ref. 40).

Acknowledgements

We thank the patients and their families for participation; E. Al-Sabban, L. Alsford, J.L. André, F. Bouissou, S. Caliskan, E. Kuwertz-Bröcking, B. Lange, J. Nauta and W. Proesmans for referring patients; V. Kalatzis and L. Heidet for critical reading of the manuscript; V. Chauvet for help with in situ hybridization; and Y. Deris for assistance with figure preparation. This study was supported in part by the Association pour l'Utilisation du Rein Artificiel and the Fondation pour la Recherche Médicale. N.B. was supported by grants from the Association Française contre les Myopathies and, subsequently, the Programme Hospitalier de Recherche Clinique.

Received 28 December 1999; accepted 8 February 2000.

1. Olson, J.L. & Schwartz, M.M. The nephrotic syndrome: minimal change disease, focal segmental glomerulosclerosis, and miscellaneous causes. in *Heptinstall's Pathology of the Kidney* (eds Jennette, J.C., Olson, J.L. & Silva, F.G.) 187–257 (Lippincott-Raven, Philadelphia, 1998).
2. Broyer, M., Meyrier, A., Niaudet, P. & Habib, R. Minimal changes and focal segmental glomerular sclerosis. in *Oxford Textbook of Clinical Nephrology* (eds Davison, A.M. *et al.*) 493–535 (Oxford University Press, Oxford, 1998).
3. Kestilä, M. *et al.* Positionally cloned gene for a novel glomerular protein—nephrin—is mutated in congenital nephrotic syndrome. *Mol. Cell* **1**, 575–582 (1998).
4. Ruotsalainen, V. *et al.* Nephrin is specifically located at the slit diaphragm of glomerular podocytes. *Proc. Natl Acad. Sci. USA* **96**, 7962–7967 (1999).
5. Holthofer, H. *et al.* Nephrin localizes at the podocyte filtration slit area and is characteristically spliced in the human kidney. *Am. J. Pathol.* **155**, 1681–1687 (1999).
6. Holzman, L.B. *et al.* Nephrin localizes to the slit pore of the glomerular epithelial cell. *Kidney Int.* **56**, 1481–1491 (1999).
7. Mathis, B.J. *et al.* A locus for inherited focal segmental glomerulosclerosis maps to chromosome 19q13. *Kidney Int.* **53**, 282–286 (1998).
8. Winn, M.P. *et al.* Linkage of a gene causing familial focal segmental glomerulosclerosis to chromosome 11 and further evidence of genetic heterogeneity. *Genomics* **58**, 113–120 (1999).
9. Fuchshuber, A. *et al.* Mapping a gene (SRN1) to chromosome 1q25–q31 in idiopathic nephrotic syndrome confirms a distinct entity of autosomal recessive nephrosis. *Hum. Mol. Genet.* **4**, 2155–2158 (1995).
10. Dib, C. *et al.* A comprehensive genetic map of the human genome based on 5,264 microsatellites. *Nature* **380**, 152–154 (1996).
11. Kozak, M. Interpreting cDNA sequences: some insights from studies on translation. *Mamm. Genome* **7**, 563–574 (1996).
12. Prestridge, D.S. Predicting Pol II promoter sequences using transcription factor binding sites. *J. Mol. Biol.* **249**, 923–932 (1995).
13. Bairoch, A., Bucher, P. & Hofmann, K. The PROSITE database, its status in 1995. *Nucleic Acids Res.* **24**, 189–196 (1996).
14. Nakai, K. & Kanehisa, M. A knowledge base for predicting protein localization sites in eukaryotic cells. *Genomics* **14**, 897–911 (1992).
15. Snyers, L., Umlauf, E. & Prohaska, R. Cysteine 29 is the major palmitoylation site on stomatin. *FEBS Lett.* **449**, 101–104 (1999).
16. Stewart, G.W. *et al.* Isolation of cDNA coding for an ubiquitous membrane protein deficient in high Na^+, low K^+ stomatocytic erythrocytes. *Blood* **79**, 1593–1601 (1992).
17. Huang, M., Gu, G., Ferguson, E.L. & Chalfie, M. A stomatin-like protein necessary for mechanosensation in C. elegans. *Nature* **378**, 292–295 (1995).
18. Mannsfeldt, A.G., Carroll, P., Stucky, C.L. & Lewin, G.R. Stomatin, a MEC-2 like protein, is expressed by mammalian sensory neurons. *Mol. Cell. Neurosci.* **13**, 391–404 (1999).
19. Salzer, U., Ahorn, H. & Prohaska, R. Identification of the phosphorylation site on human erythrocyte band 7 integral membrane protein: implications for a monotopic protein structure. *Biochim. Biophys. Acta.* **1151**, 149–152 (1993).
20. Snyers, L., Umlauf, E. & Prohaska, R. Oligomeric nature of the integral membrane protein stomatin. *J. Biol. Chem.* **273**, 17221–17226 (1998).
21. Engelman, J.A., Zhang, X.L., Razani, B., Pestell, R.G. & Lisanti, M.P. p42/44 MAP kinase-dependent and -independent signaling pathways regulate caveolin-1 gene expression. *J. Biol. Chem.* **274**, 32333–32341 (1999).
22. Shih, N.Y. *et al.* Congenital nephrotic syndrome in mice lacking CD2-associated protein. *Science* **286**, 312–315 (1999).
23. Kirsch, K.H., Georgescu, M.M., Ishimaru, S. & Hanafusa, H. CMS: an adapter molecule involved in cytoskeletal rearrangements. *Proc. Natl Acad. Sci. USA* **96**, 6211–6216 (1999).
24. Noakes, P.G. *et al.* The renal glomerulus of mice lacking s-laminin/laminin β2: nephrosis despite molecular compensation by laminin β1. *Nature Genet.* **10**, 400–406 (1995).
25. Parving, H.H. *et al.* Prevalence and causes of albuminuria in non-insulin-dependent diabetic patients. *Kidney Int.* **41**, 758–762 (1992).
26. Connolly, J.O., Weston, C.E. & Hendry, B.M. HIV-associated renal disease in London hospitals. *Q. J. Med.* **88**, 627–634 (1995).
27. Verani, R.R. Obesity-associated focal segmental glomerulosclerosis: pathological features of the lesion and relationship with cardiomegaly and hyperlipidemia. *Am. J. Kidney Dis.* **20**, 629–634 (1992).
28. Ioannou, P.A. *et al.* A new bacteriophage P1-derived vector for the propagation of large human DNA fragments. *Nature Genet.* **6**, 84–89 (1994).
29. Trask, B.J. *et al.* Characterization of somatic cell hybrids by bivariate flow karyotyping and fluorescence in situ hybridization. *Somat. Cell Mol. Genet.* **17**, 117–136 (1991).
30. Town, M. *et al.* A novel gene encoding an integral membrane protein is mutated in nephropathic cystinosis. *Nature Genet.* **18**, 319–324 (1998).
31. Li, B.L. *et al.* Human acyl-CoA:cholesterol acyltransferase-1 (ACAT-1) gene organization and evidence that the 4.3-kilobase ACAT-1 mRNA is produced from two different chromosomes. *J. Biol. Chem.* **274**, 11060–11071 (1999).
32. Brandenberger, A.W., Tee, M.K., Lee, J.Y., Chao, V. & Jaffe, R.B. Tissue distribution of estrogen receptors α (ER-α) and β (ER-β) mRNA in the midgestational human fetus. *J. Clin. Endocrinol. Metab.* **82**, 3509–3512 (1997).
33. Altschul, S.F., Gish, W., Miller, W., Myers, E.W. & Lipman, D.J. Basic local alignment search tool. *J. Mol. Biol.* **215**, 403–410 (1990).
34. Thompson, J.D., Higgins, D.G. & Gibson, T.J. CLUSTAL W: improving the sensitivity of progressive multiple sequence alignment through sequence weighting, position-specific gap penalties and weight matrix choice. *Nucleic Acids Res.* **22**, 4673–4680 (1994).
35. Fuchshuber, A. *et al.* Presymptomatic diagnosis of familial steroid-resistant nephrotic syndrome. *Lancet* **347**, 1050–1051 (1996).
36. Sibony, M., Commo, F., Callard, P. & Gasc, J.M. Enhancement of mRNA *in situ* hybridization signal by microwave heating. *Lab. Invest.* **73**, 586–591 (1995).
37. Kalatzis, V., Sahly, I., El-Amraoui, A. & Petit, C. Eya1 expression in the developing ear and kidney: towards the understanding of the pathogenesis of branchio-oto-renal (BOR) syndrome. *Dev. Dyn.* **213**, 486–499 (1998).
38. Heidet, L. *et al.* Diffuse leiomyomatosis associated with X-linked Alport syndrome: extracellular matrix study using immunohistochemistry and in situ hybridization. *Lab. Invest.* **76**, 233–243 (1997).
39. Antonarakis, S.E. Recommendations for a nomenclature system for human gene mutations. Nomenclature Working Group. *Hum. Mutat.* **11**, 1–3 (1998).
40. Kaplan, J.M. *et al.* Mutations in ACTN4, encoding a-actinin 4, cause familial focal segmental glomerulosclerosis. *Nature Genet.* **64**, 251–256 (2000).